

# Tau accumulates in synaptogyrin-3 positive synapses in Progressive Supranuclear Palsy

Robert McGeachan<sup>1</sup>, Maxwell P Spires-Jones<sup>1</sup>, Mollie Gilmore<sup>1</sup>, Jamie Rose<sup>1</sup>,  
Tara L Spires-Jones<sup>#1</sup>

<sup>1</sup> The University of Edinburgh Centre for Discovery Brain Sciences and UK Dementia Research Institute, Edinburgh.

# Correspondence to  
Prof Tara Spires-Jones  
[Tara.spires-jones@ed.ac.uk](mailto:Tara.spires-jones@ed.ac.uk)  
Centre for Discovery Brain Sciences  
The University of Edinburgh  
1 George Square, Edinburgh EH8 9JZ, UK

Keywords:

Progressive supranuclear palsy, tauopathy, tau, synapse, synaptogyrin, array tomography

## Abstract

---

Synaptic function is essential for cognition and loss of synapses is observed in neurodegenerative tauopathies including Progressive Supranuclear Palsy (PSP). Accumulation of tau within presynaptic terminals has been observed in animal models expressing human tau and in Alzheimer's disease brain which contains both tau and amyloid pathologies. Tau binding to the synaptic vesicle protein synaptogyrin-3 causes presynaptic dysfunction in flies and mice, and tau colocalised with synaptogyrin-3 has been observed in human Alzheimer's disease post-mortem brain tissue, making this protein-protein interaction a promising therapeutic target. Whether this tau-synaptogyrin-3 interaction occurs in the primary tauopathy PSP remains unknown. In this study, we used high resolution array tomography imaging to examine over 30,000 synapses in post-mortem PSP and control frontal cortex tissue (7 donors per group). Using linear mixed effects modelling of the data, we observe tau protein colocalised with synaptogyrin-3 in PSP significantly more than in controls (6-fold increase,  $t=2.51$ ,  $p=0.04$ ). These data indicate that tau binding synaptogyrin-3 may induce synaptic dysfunction in PSP.

## Introduction

Synapse loss is a common phenotype in neurodegenerative disorders. In Alzheimer's disease (AD), the most common neurodegenerative disease, synapse degeneration is the strongest pathological correlate of cognitive decline and is thought to be an early feature of disease pathogenesis<sup>1</sup>. Both amyloid beta, which accumulates in amyloid plaques in AD and tau protein which accumulates in neurofibrillary tangles also accumulate within synaptic terminals where they have been linked to synaptic dysfunction and death<sup>2</sup>. A large body of evidence from ourselves and others links soluble amyloid beta to synapse degeneration in AD<sup>3-6</sup>. Similarly, accumulation of tau in synapses has been associated by many groups with synaptic dysfunction and loss in AD and model systems<sup>7-10</sup>. Since AD has other pathologic hallmarks, and tau pathology in AD is likely preceded and potentiated by extracellular amyloid-beta (A $\beta$ ) pathology, AD is considered a "secondary" tauopathy<sup>11</sup>.

Primary tauopathies are disorders in which tau aggregation is thought to be the primary cause of neurodegeneration alone. Primary tauopathies include progressive supranuclear palsy (PSP – the most common), frontotemporal dementia with Parkinsonism linked to chromosome 17 (FTDP-17) and corticobasal degeneration (CBD) among others<sup>12</sup>. The canonical function of the tau protein involves microtubule stabilisation; however recent data suggest tau has multiple other physiological roles including in synaptic plasticity and cognition<sup>13</sup>. In tauopathies, tau becomes hyperphosphorylated, misfolded, and aggregates in the somatodendritic compartment.

In PSP patients there is synaptic loss in the frontal cortex<sup>14</sup>, and cross-sectional PET data have demonstrated an association between synaptic density, tau burden and disease severity<sup>15</sup>. However, it is currently unknown if tau accumulates within synapses in PSP. In AD and *Drosophila* and mouse models of tauopathy, we have observed that tau within presynaptic terminals where it colocalises with the presynaptic vesicle protein synaptogyrin-3<sup>16-18</sup>. In the model systems, lowering synaptogyrin-3 levels prevented synapse loss and memory decline, indicating that disrupting this protein-protein interaction is a promising therapeutic avenue to prevent synaptic dysfunction, loss, and downstream cognitive deficits. In this study, we tested the hypotheses that tau accumulates in presynaptic terminals in PSP and that it accumulates with synaptogyrin-3.

## Methods

### Subjects

Post-mortem human brain tissue was acquired from the Edinburgh Sudden Death Brain Bank/ Alzheimer's Scotland Brain and Tissue Bank (research ethics committee approval 16/ES/0084). 7 PSP and 7 Control cases were included in analysis (**Table 1**). Inclusion criteria for PSP were a neuropathological diagnosis of PSP and clinical diagnosis of progressive neurodegeneration. Exclusion criteria for control cases included known clinical neurological or psychiatric disease or a neuropathological report consistent with tauopathy. Case information was blinded during image processing and analysis. The individual case information and demographics are shown in Table 1. Experiments were approved by the Edinburgh Brain Bank ethics committee, the Academic and Clinical Central Office for Research and Development (ACCORD) and the medical research ethics committee AMREC a joint office of the University of Edinburgh and National Health Service Lothian, approval number 15-HV-016). The study size was based on available tissue embedded for array tomography. Case ID numbers are provided as required by our ethical approval from the MRC and Edinburgh brain banks. All data has been pseudoanonymized so personal identifying information cannot be accessed with these numbers.

| Diagnosis | Case ID<br>MRC | Case ID<br>Edinburgh | Age | Sex | PMI<br>(h) | Brain Weight<br>(g) | Brain pH |
|-----------|----------------|----------------------|-----|-----|------------|---------------------|----------|
| PSP       | 001.32816      | SD006/18             | 70s | M   | 114        | 1309                | 6.0      |
| PSP       | 001.36418      | SD008/21             | 60s | F   | 62         | 1036                | 6.21     |
| PSP       | 001.35381      | SD009/19             | 70s | M   | 66         | 1242                | 6.19     |
| PSP       | 001.30843      | SD030/17             | 70s | M   | 46         | 1477                | 6.12     |
| PSP       | 001.30855      | SD033/17             | 80s | M   | 89         | 1197                | 6.15     |
| PSP       | 001.32508      | SD049/17             | 60s | M   | 79         | 1325                | 6.0      |
| PSP       | 001.36927      | SD041/21             | 70s | M   | 103        | 1457                | 5.95     |
| Control   | 001.29880      | SD010/17             | 50s | M   | 64         | 1520                | 6.41     |
| Control   | 001.28794      | SD017/16             | 70s | F   | 72         | 1219                | 5.95     |
| Control   | 001.26495      | SD024/15             | 70s | M   | 39         | 1290                | 6.17     |
| Control   | 001.28797      | SD025/16             | 70s | M   | 57         | 1301                | 6.11     |
| Control   | 001.35529      | SD026/19             | 50s | M   | 96         | 1650                | 6.49     |
| Control   | 001.29084      | SD032/16             | 50s | M   | 104        | 1560                | 6.14     |
| Control   | 001.28402      | SD051/15             | 70s | M   | 49         | 1503                | 6.33     |

**Table 1:** Participant details. PMI = post-mortem interval.

### Array Tomography tissue preparation and staining

Samples from the frontal cortex (Brodmann area 9, BA9), were fixed and embedded for array tomography as described previously<sup>19</sup>. Briefly, fresh tissue samples (~1cm<sup>3</sup>) were fixed in 4% paraformaldehyde for 3 hours, dehydrated in ethanol and incubated in LR White resin overnight at 4°C. Individual samples were cured in LR White in gelatin capsules overnight at 53°C. Two individual sample blocks were used from each case, each in a separate staining session. Embedded samples were cut into ribbons of ultrathin serial 70 nm sections using a histo Jumbo Diamond knife (Diatome) and an Ultracut (Leica). Ribbons were mounted on gelatin-coated glass coverslips and dried on a slide warmer. Coverslips were subjected to citric acid (pH6) antigen retrieval with 2 minutes of boiling on the steam setting in a pressure cooker. Sections were washed with water, dried, and the ribbons of sections outlined with hydrophobic pen. Ribbons were rehydrated in 50 mM glycine (10 min) and blocked in a solution of 0.1% fish skin gelatin and 0.05% Tween in TBS for 30 minutes at room temperature. Ribbons were incubated with primary antibodies diluted in blocking buffer overnight at 4 °C. Primary antibodies were to human tau (R&D systems AF3494, raised in goat, 1:50 dilution) and synpatogyrin-3 (Santa Cruz sc-271046, raised in mouse, 1:25 dilution). and synaptophysin (Abcam ab196379, raised in rabbit, 1:50 dilution). Ribbons were washed with TBS followed by incubation with secondary antibodies diluted 1:200 in blocking solution for 30 minutes at room temperature (AlexaFluor 405 labelled donkey anti-goat, Abcam Ab1756 and AlexaFluor 594 labelled donkey anti-mouse IgG1, Invitrogen A21203). Ribbons were then washed with TBS and incubated in directly labelled 488 synaptophysin antibody (Abcam ab196379) diluted in blocking solution (1:50) for 1 hour at room temperature. Ribbons were then washed with TBS and distilled water before mounting on glass slides with ImmuMount (Thermo). A negative control with no primary antibodies and a positive control for tau staining using a ribbon from temporal cortex of a Braak VI AD case were performed in each experiment.

### Microscopy and Image Analysis

Images were acquired using Zen software on a Zeiss AxioImager Z2 using a 63x oil immersion objective (1.4 numerical aperture) and a CoolSnap digital camera. Two regions of interest (ROIs) were chosen in the gray matter of BA9 and imaged in the same location on 15-30 sequential sections using cell bodies as fiduciary markers to locate the ROI. Exposure settings were determined using a ribbon from an AD case stained as above to ensure copious tau pathology was present for determining optimal exposure times. Imaging parameters were kept the same throughout the imaging batch, and an image was taken of the negative control in each session to ensure there was not non-specific staining.

Before image processing, experimenters were blinded to case information. Individual images from each ROI were combined into a 3D image stack and a median background filter was applied in Image J with custom batch macros. Using custom MATLAB scripts, image stacks were aligned using rigid registration. Each channel was segmented using an auto-local thresholding algorithm to binarize images and remove any objects present in only a single section (from secondary antibody noise). Segmented images were run through custom MATLAB and Python scripts to determine object density and colocalization between channels. Objects were considered colocalized if at least 25% of the volume overlapped. All custom software scripts are available on GitHub <https://github.com/Spires-Jones-Lab>.

## Statistical analyses

Statistical analyses were performed using RStudio. Distributions of demographic data were assessed using inspection of histograms and Shapiro-Wilks tests resulting in the choice of non-parametric tests to compare groups. For array tomography analyses, linear mixed effects model (lme4 R package) were used with disease as a fixed effect and block nested in case as a random effect to avoid pseudoreplication of the data. Assumptions of the models were tested by examining residual plots and performing Shapiro-Wilks tests on residuals of the models. Where the model did not fit test assumptions, data were transformed using a Tukey transformation and the models run again. The statistical analysis script and data spreadsheets are available as supplemental data.

## Results

### Participant demographics

Post-mortem samples of frontal cortex were examined from 7 PSP and 7 matched control cases. Examining the demographic data from the participants confirms that control and PSP cases were not significantly different in age (Wilcoxon test,  $W=91$ ,  $p=0.38$ ), sex (Fischer's exact test,  $p = 0.67$ ) or PMI (Wilcoxon test,  $W=200$   $p = 0.08$ ). Brain weight was significantly lower in PSP than control cases as expected due to progressive neurodegeneration (Wilcoxon test,  $W=176$ ,  $p=0.01$ , **Table 2**).

|                                     | Control<br>(N=7)  | PSP<br>(N=7)      |
|-------------------------------------|-------------------|-------------------|
| <b>Age (Years)</b>                  |                   |                   |
| Mean (SD)                           | 69.7 (11.3)       | 71.6 (6.43)       |
| Median [Min, Max]                   | 78.0 [57.0, 79.0] | 73.0 [61.0, 81.0] |
| <b>Sex</b>                          |                   |                   |
| M                                   | 6 (85.7%)         | 6 (85.7%)         |
| F                                   | 1 (14.3%)         | 1 (14.3%)         |
| <b>brain pH</b>                     |                   |                   |
| Mean (SD)                           | 6.23 (0.189)      | 6.09 (0.104)      |
| Median [Min, Max]                   | 6.17 [5.95, 6.49] | 6.12 [5.95, 6.21] |
| <b>post-mortem interval (hours)</b> |                   |                   |
| Mean (SD)                           | 68.7 (23.9)       | 79.9 (24.0)       |
| Median [Min, Max]                   | 64.0 [39.0, 104]  | 79.0 [46.0, 114]  |
| <b>* Brain weight (g)</b>           |                   |                   |
| Mean (SD)                           | 1430 (163)        | 1290 (153)        |
| Median [Min, Max]                   | 1500 [1220, 1650] | 1310 [1040, 1480] |

**Table 2: Case demographics summary by diagnosis.** \*  $p=0.01$  Wilcoxon test.

## Tau is found colocalised with synaptogyrin-3 in PSP

We examined the colocalization of synaptogyrin-3 and tau in synapses using an array tomography workflow (**Figure 1**). In this workflow, brain samples are embedded in resin sectioned into ribbons of serial ultrathin 70nm sections, immunostained, imaged, and images are processed to align the images, segment them, and remove background noise present in single sections before determining object numbers and colocalization in three-dimensions.

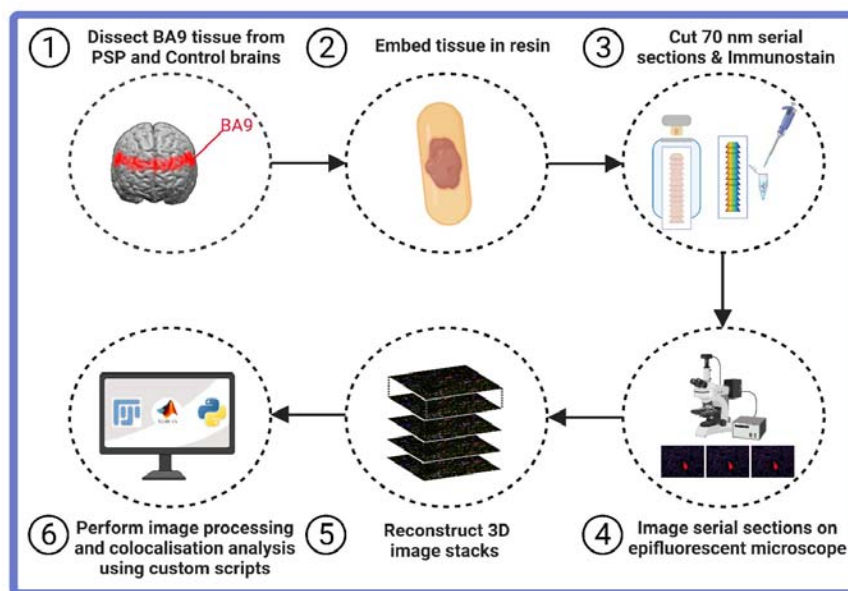


**Figure 1: Array tomography workflow.** Created with BioRender.com

Examination of the array tomography image stacks reveals substantial colocalization of synaptophysin and synaptogyrin-3 as expected since these are both found on presynaptic vesicles (**Figure 2**). In PSP cases, rare synapses are observed to be colocalised with tau. Quantification of these images reveals that the percentage of synaptogyrin-3 positive puncta in PSP cases contained 6-fold more tau than control cases (0.16% of synaptogyrin puncta contain tau in PSP cases and 0.03% in control cases). This is a significant increase as assessed by a linear mixed effects model of Tukey transformed data with diagnosis as the dependent variable and block nested in case as a random effect (**Figure 3A**,  $t=2.25$ ,  $p=0.044$ ). Similarly, the percentage of synaptophysin puncta containing tau was significantly higher in PSP cases (**Figure 3B**,  $t=2.24$ ,  $p=0.047$ ). As expected, the burden of tau pathology assessed as the



percentage volume occupied by tau staining was significantly higher in PSP cases (**Figure 3C**,  $t=5.73$ ,  $p<0.0001$ ). The proportion of synaptogyrin-3 puncta containing tau positively correlated with the tau burden in PSP cases (**Figure 3D**, Spearman correlation  $\rho=4$ ,  $p=0.007$ ) but not in control cases (Spearman correlation  $\rho=15.41$ ,  $p=0.71$ ).

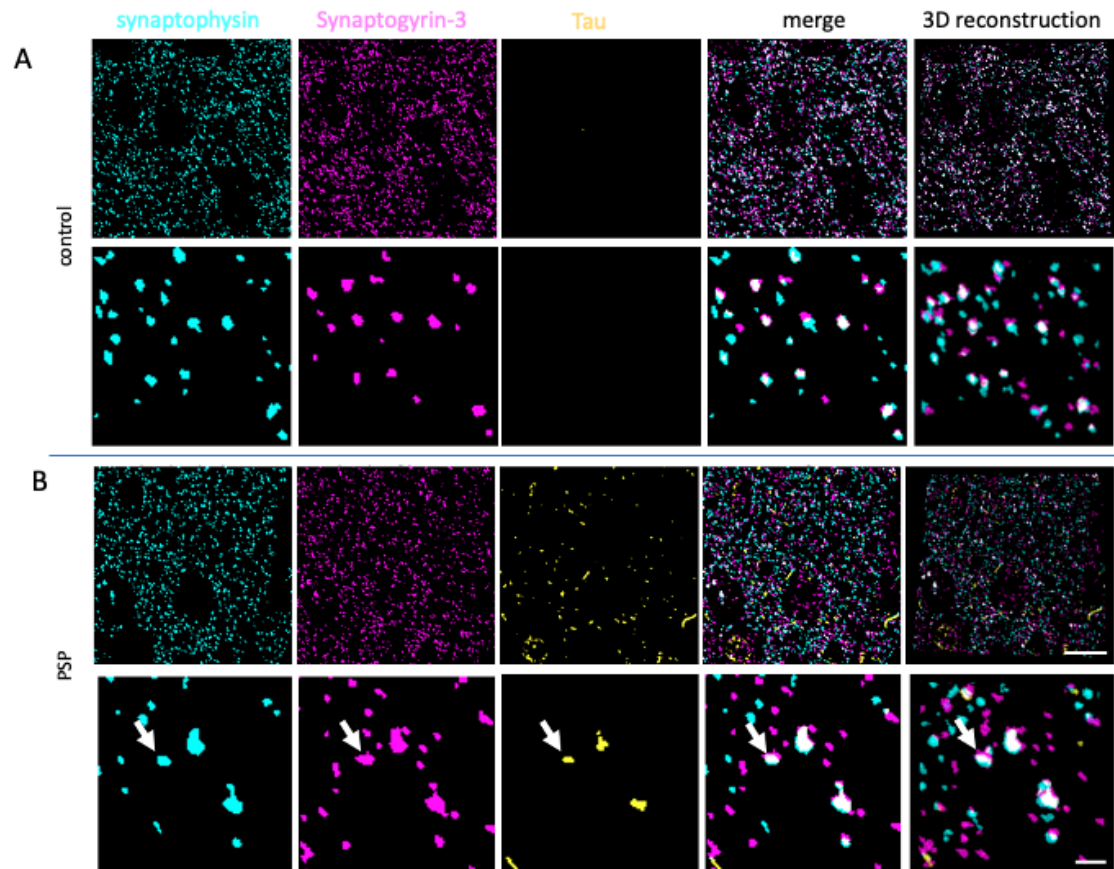


**Figure 2: Segmented array tomography images.** Array tomography ribbons were stained for synaptophysin (cyan), synaptogyrin-3 (magenta) and tau (yellow). Representative images of maximum intensity z-projections of 5 serial sections are shown for a control (A) and a PSP case (B). The top row of each panel contains a 50x50  $\mu\text{m}$  region of interest with a 10  $\mu\text{m}$  scale bar and the bottom rows contain a zoomed-in 10x10  $\mu\text{m}$  region of interest with a 2  $\mu\text{m}$  scale bar. The far right column shows three-dimensional reconstructions of 5 serial sections. An arrow indicates a synapse containing tau in the PSP case.

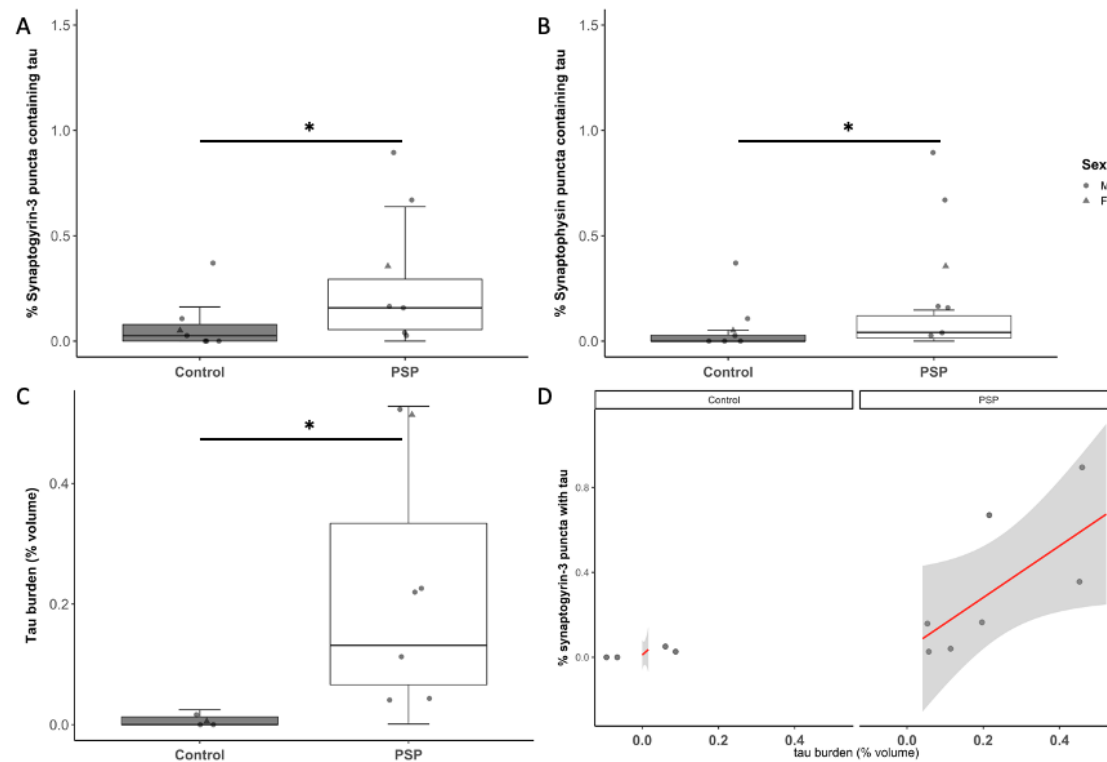


**Figure 3: Increased synaptic tau and colocalization with synaptogyrin-3 in PSP.** Quantification of segmented array tomography images reveals increases in the percentage of synaptogyrin-3 puncta containing tau (A), synaptophysin puncta containing tau (B), and increased tau burden (C). Tau burden positively correlates with the percentage of synaptogyrin-3 puncta containing tau in PSP but not control cases (D).

## Discussion

Synaptic dysfunction is an early event associated with tau pathology in animal models of tauopathy, and synapses are lost in human tauopathies including PSP<sup>2,15</sup>. Previous studies have demonstrated that tau and synaptogyrin-3 interact in animal models, causing clustering of synaptic vesicles, synapse loss, and cognitive impairment<sup>16–18</sup>. Further, in human Alzheimer's disease brain, a secondary tauopathy, we previously observed tau colocalised with synaptogyrin-3<sup>16</sup>.

This study reveals that in PSP, there are a subset of synapses positive for synaptogyrin-3 and synaptophysin that contain tau protein. While the percentage of tau containing synapses is small (less than 0.5%), the sheer number of synapses in the brain means that even a small proportion of affected synapses may still have a biologically meaningful effect. Our data together with the preceding animal work

showing functional recovery with lowering synaptogyrin-3 levels in tau models together indicate that in primary tauopathies as well as AD, tau-synaptogyrin-3 interactions may be important for synaptic dysfunction and loss and thus stopping this interaction is a potential therapeutic target to save synapses.

## Acknowledgements

We gratefully acknowledge the contributions of our brain tissue donors and their families. This work was supported by the UK Dementia Research Institute which receives its funding from DRI Ltd, funded by the UK Medical Research Council, Alzheimer's Society, and Alzheimer's Research UK. RM is funded by a Wellcome Trust Clinical Academic PhD studentship. The confocal microscope was generously funded by Alzheimer's Research UK and a Wellcome Trust Institutional Strategic Support Fund at the University of Edinburgh.

## Data Availability Statement

Upon acceptance of the peer-reviewed version of this manuscript, all data spreadsheets and statistical analysis files will be available online as supplementary data. Images are available upon reasonable request. All custom software and scripts used in the study is available on GitHub at <https://github.com/Spires-Jones-Lab>

## Competing Interests

TLS-J receives funding as a scientific advisory board member/scientific consultant from Cognition Therapeutics and Jay Therapeutics.

## References

1. Colom-Cadena M, Spires-Jones T, Zetterberg H, et al. The clinical promise of biomarkers of synapse damage or loss in Alzheimer's disease. *Alzheimers Res Ther*. 2020;12(1):21. doi:10.1186/s13195-020-00588-4
2. Spires-Jones TL, Hyman BT. The intersection of amyloid beta and tau at synapses in Alzheimer's disease. *Neuron*. 2014;82(4):756-771. doi:10.1016/j.neuron.2014.05.004
3. Koffie RM, Meyer-Luehmann M, Hashimoto T, et al. Oligomeric amyloid beta associates with postsynaptic densities and correlates with excitatory synapse loss near senile plaques. *Proc Natl Acad Sci U S A*. 2009;106(10):4012-4017. doi:10.1073/pnas.0811698106

4. Hong W, Wang Z, Liu W, et al. Diffusible, highly bioactive oligomers represent a critical minority of soluble A $\beta$  in Alzheimer's disease brain. *Acta Neuropathol.* 2018;136(1):19-40. doi:10.1007/s00401-018-1846-7
5. Koffie RM, Hashimoto T, Tai HC, et al. Apolipoprotein E4 effects in Alzheimer's disease are mediated by synaptotoxic oligomeric amyloid- $\beta$ . *Brain.* 2012;135(Pt 7):2155-2168. doi:10.1093/brain/aww127
6. Li S, Selkoe DJ. A mechanistic hypothesis for the impairment of synaptic plasticity by soluble A $\beta$  oligomers from Alzheimer's brain. *J Neurochem.* 2020;154(6):583-597. doi:10.1111/jnc.15007
7. Lasagna-Reeves CA, Castillo-Carranza DL, Sengupta U, Clos AL, Jackson GR, Kayed R. Tau oligomers impair memory and induce synaptic and mitochondrial dysfunction in wild-type mice. *Molecular Neurodegeneration.* 2011;6(1):39. doi:10.1186/1750-1326-6-39
8. Kopeikina KJ, Hyman BT, Spires-Jones TL. Soluble forms of tau are toxic in Alzheimer's disease. *Transl Neurosci.* 2012;3(3):223-233. doi:10.2478/s13380-012-0032-y
9. Pickett EK, Henstridge CM, Allison E, et al. Spread of tau down neural circuits precedes synapse and neuronal loss in the rTgTauEC mouse model of early Alzheimer's disease. *Synapse.* 2017;71(6). doi:10.1002/syn.21965
10. Pickett EK, Herrmann AG, McQueen J, et al. Amyloid Beta and Tau Cooperate to Cause Reversible Behavioral and Transcriptional Deficits in a Model of Alzheimer's Disease. *Cell Rep.* 2019;29(11):3592-3604.e5. doi:10.1016/j.celrep.2019.11.044
11. Gomes LA, Hipp SA, Rijal Upadhaya A, et al. A $\beta$ -induced acceleration of Alzheimer-related  $\tau$ -pathology spreading and its association with prion protein. *Acta Neuropathologica.* 2019;138(6):913-941. doi:10.1007/s00401-019-02053-5
12. Kovacs GG. Tauopathies. In: *Handbook of Clinical Neurology.* Vol 145. Elsevier B.V.; 2018:355-368. doi:10.1016/B978-0-12-802395-2.00025-0
13. Kent SA, Spires-Jones TL, Durrant CS. The physiological roles of tau and A $\beta$ : implications for Alzheimer's disease pathology and therapeutics. *Acta Neuropathol.* 2020;140(4):417-447. doi:10.1007/s00401-020-02196-w
14. Bigio EH, Vono MB, Satumtira S, et al. Cortical Synapse Loss in progressive Supranuclear palsy. *Journal of Neuropathology & Experimental Neurology.* 2001;60(5):403-410. doi:10.1093/jnen/60.5.403
15. Holland N, Malpetti M, Rittman T, et al. Molecular pathology and synaptic loss in primary tauopathies: an 18F-AV-1451 and 11C-UCB-J PET study. *Brain.* 2022;145(1):340-348. doi:10.1093/brain/awab282
16. Largo-Barrientos P, Apóstolo N, Creemers E, et al. Lowering Synaptogyrin-3 expression rescues Tau-induced memory defects and synaptic loss in the

presence of microglial activation. *Neuron*. Published online January 7, 2021.  
doi:10.1016/j.neuron.2020.12.016

17. McInnes J, Wierda K, Snellinx A, et al. Synaptogyrin-3 Mediates Presynaptic Dysfunction Induced by Tau. *Neuron*. 2018;97(4):823-835.e8.  
doi:10.1016/j.neuron.2018.01.022
18. Zhou L, McInnes J, Wierda K, et al. Tau association with synaptic vesicles causes presynaptic dysfunction. *Nat Commun*. 2017;8:15295.  
doi:10.1038/ncomms15295
19. Kay KR, Smith C, Wright AK, et al. Studying synapses in human brain with array tomography and electron microscopy. *Nature Protocols*. 2013;8(7):1366-1380.  
doi:10.1038/nprot.2013.078